MIT Libraries | DSpace@MIT

MIT Open Access Articles

Piezoelectric transducer based miniature catheter for ultrahigh speed endoscopic optical coherence tomography

Citation: Tsai, Tsung-Han et al. "Piezoelectric Transducer Based Miniature Catheter for Ultrahigh Speed Endoscopic Optical Coherence Tomography." Proc. SPIE 7889, 788919 (2011). © 2011 Copyright SPIE

As Published: http://dx.doi.org/10.1117/12.875815

Publisher: SPIE

Persistent URL: http://hdl.handle.net/1721.1/71929

Version: Final published version: final published article, as it appeared in a journal, conference proceedings, or other formally published context

Massachusetts Institute of Technology

Piezoelectric Transducer Based Miniature Catheter for Ultrahigh Speed Endoscopic Optical Coherence Tomography

Tsung-Han Tsai[1], Benjamin M. Potsaid[1,2], Martin Kraus[1,3], Jonathan J. Liu[1], Chao Zhou[1], Joachim Hornegger[3], and James G. Fujimoto[1]

[1]Department of Electrical Engineering & Computer Science and Research Laboratory of Electronics, Massachusetts Institute of Technology, Cambridge, MA
[2]Advanced Imaging Group, Thorlabs, Inc., Newton, NJ
[3]Pattern Recognition Lab, University Erlangen-Nuremberg, Erlangen, Germany

Abstract

We developed a piezoelectric transducer (PZT) based miniature catheter with an outer diameter of 3 mm for ultrahigh speed endoscopic optical coherence tomography (OCT) using Fourier domain modelocked (FDML) laser at a 480 kHz axial scan rate. The miniaturized PZT bender actuates a fiber to provide high scanning speed. The side-viewing probe can be pulled back for a long distance to acquire three-dimensional (3D) dataset covering a large area on the specimen. Operating with a high speed data acquisition (DAQ) system, OCT imaging with 6.5 mm imaging range, 10 μm axial resolution, 20 μm lateral resolution, and frame rate of 480 frames per second (fps) is demonstrated.

Introduction

Optical coherence tomography (OCT) performs micrometer-scale, cross-sectional imaging by measuring the echo time delay of the backscattered light[1]. Internal body imaging was enabled by the development of fiber-optics based OCT endoscopes[2, 3]. *In vivo* endoscopic OCT imaging is very challenging because fast optical scanning must be implemented inside a small imaging probe. Many scanning mechanisms have been realized in catheter based endoscopic OCT systems, such as rotating a fiber micro-prism module at the proximal end[2, 4-6], swinging the distal fiber tip by a galvanometric plate[7], swinging the cantilever fiber by piezoelectric actuators[8, 9], and scanning the beam using microelectromechenical systems[10-13]. Although these endoscopic OCT imaging techniques potentially can achieve very high imaging speed, to date, none of them has been demonstrated over 100 fps due to other hardware limitations such as the speed of rotation for the optics or limitations in the OCT acquisition rate. Recently record imaging speeds have been demonstrated in a microscopy system using multiple scanning spots and a buffered Fourier domain modelocked (FDML) laser [14]. However ultrafast imaging speeds have not yet been demonstrated endoscopically.

In this paper we demonstrate a piezoelectric transducer (PZT) based miniature catheter with an outer diameter of 3mm for ultrahigh speed endoscopic OCT imaging. The combination of miniaturized PZT bender and cantilever fiber has the advantage of large deflection with low driving voltage, ease of adjustment of the scanning frequency, and flexibility to implement the slow scan methods to achieve three-dimensional imaging. The side-viewing probe can be pulled back over a long distance to acquire three-dimensional (3D) datasets covering a large area on the specimen. A 480 kHz axial scan rate from an FDML laser provides high frame rate while maintaining sufficient lines per frame. Using a high speed data acquisition (DAQ) system, ultrahigh speed endoscopic OCT imaging can be achieved and large volume datasets can be acquired in seconds.

Methods

Figure 1 shows the schematic diagram of the PZT based catheter design. A tapered PZT bender with length of 15 mm and width tapered from 1.5 mm to 0.95 mm was used to deflect the fiber. UV cured epoxy was used to fix the fiber

at the distal end of the PZT bender to support cantilever vibration. The fiber tip was angle cleaved with 8 degree to reduce backreflection. The scanning fiber tip is imaged onto the tissue with a GRIN lens of 0.25 pitch (N.A. = 0.46) and 1.8 mm diameter. The working distance and the focus spot size are adjustable by changing the distance between the fiber tip and the GRIN lens. A micro-prism with size of 1mm x 1mm was glued on the distal end of the GRIN lens to reflect the laser beam to the side. In this study, the lateral scanning range of the imaging beam is about 2.5mm with the PZT bender driven with a voltage of 25 V (peak to peak). A thin holder is used to fix the PZT bender and a torque coil with 2.2 mm outer diameter. The torque coil can translate in a slow scan driven by a motor at the proximal end of the catheter. The inlet shows the photo of the prototype probe.
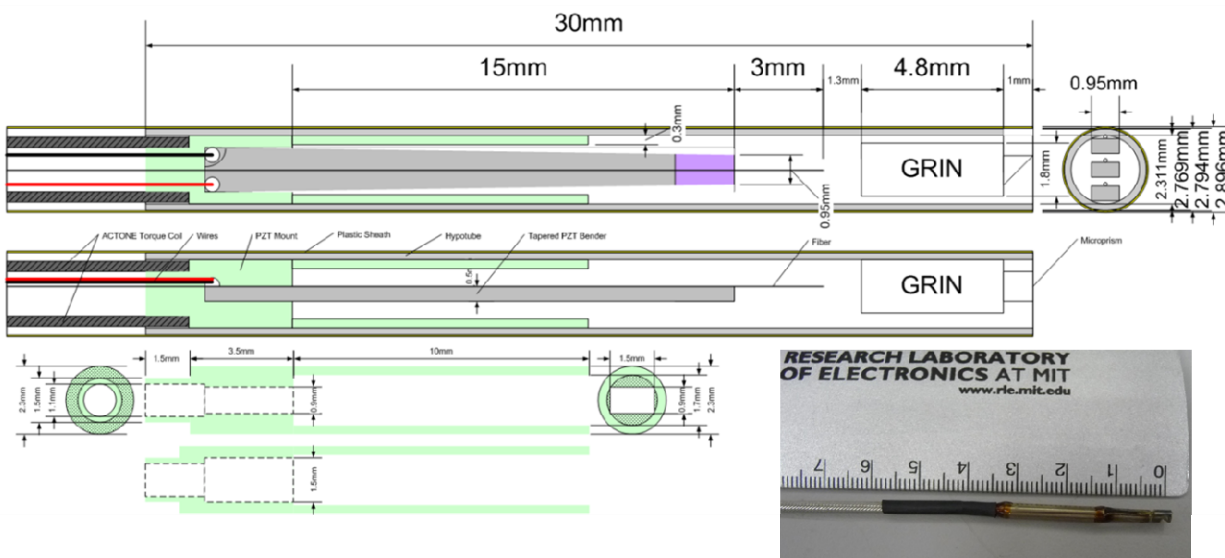

Figure 1. Schematic diagrams of the PZT probe and the photo of the prototype probe.

In this study, two FDML lasers were used to demonstrate the high speed OCT imaging. Fig. 2 (A) shows a schematic of the double-buffered FDML laser for the endoscopic OCT system[4]. The laser is a ring resonator geometry with two optical isolators (ISO), a semiconductor optical amplifier (SOA) as the gain medium, and a tunable filter (FFP-TF) in a cavity. The FFP-TF is driven with a sinusoidal waveform at 58.9 kHz, synchronous to the optical round-trip time of the 3,452 m long cavity. Two copies of the backward sweeps are extracted at evenly-spaced points within the cavity using 80/20 and 70/30 fiber-optic splitters. These copies are again split, copied, time delayed by 4 µs, and recombined in the external buffering stage. The average output power after the booster amplifier was 60mW. Fig. 2 (B) shows the output spectra of the FDML laser. The central wavelength is ~1315 nm. The total tuning range of the spectrum is 175 nm, with an 112 nm full width half maximum (FWHM). Fig. 2 (C) shows the instantaneous fringe trace from a Mach-Zehnder interferometer. The duration of each sweep is 4 µs. The duty cycle of the laser sweeps are almost 100%. The 3 copies of the sweeps are almost identical. Fig. 2 (D) shows a schematic of the triple-buffered FDML laser for the endoscopic OCT system. Similar to the 240 kHz FDML laser shown in Fig. 2 (A), the FFP-TF is driven with a sinusoidal waveform at 59.8 kHz, synchronous to the optical round-trip time of the 3,436 m long cavity. Two copies of the backward sweeps are extracted at evenly-spaced points within the cavity using 80/20 and 70/30 fiber-optic splitters. These copies are again split, copied, time delayed by 4µs, and recombined in the external buffering stage. To achieve effective sweep rate of 480 kHz, an additional external buffering stage is added to again double the effective sweep rate of the FDML laser. The average output power after the booster amplifier was 40 mW. Fig. 2 (E) shows the output spectra of the FDML laser. The central wavelength is ~1315nm. The total tuning range of the spectrum is 150 nm, with an 80 nm full width half maximum (FWHM). Fig. 2 (F) shows the instantaneous fringe trace from a Mach-Zehnder

interferometer. The duration of each sweep is 2 μs. The duty cycle of the laser sweeps are almost 100%. The 7 copies of the sweeps are almost identical.
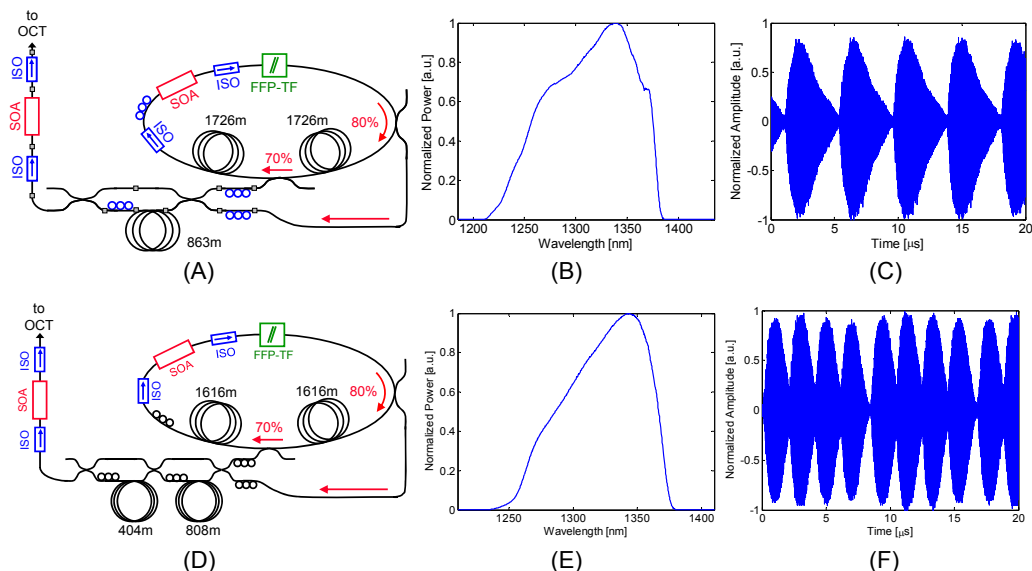

Figure 1. (A) Schematic diagrams of the 240 kHz double-buffered FDML laser. (B) Optical spectrum of the 240 kHz laser. (C) Interferometric trace of the 240 kHz laser from the Mach-Zehnder interferometer. (D) Schematic diagrams of the 480 kHz double-buffered FDML laser. (E) Optical spectrum of the 480 kHz laser. (F) Interferometric trace of the 480 kHz laser from the Mach-Zehnder interferometer.

The ultrahigh speed OCT imaging system can acquire large datasets with only a few second acquisition times. In order to support datasets greater than the 4 Gigabyte, the instrument control computer used a 64 bit operation system. The high speed A/D card can sample up to 400 MSPS at 14 bit resolution. A custom user interface and data acquisition software was developed in C++ to coordinate instrument control and enable user interaction. Improved imaging performance was obtained by modifying a commercially available 350 MHz InGaAs dual balanced detector to increase the transimpedance gain by 2X and reduce the bandwidth to 200 MHz. The imaging system thus can achieve up to 16 mm imaging range with 480 kHz axial scan rate and 480 frames per second with 500 lines per frame.

Results

The axial and transverse resolutions using this catheter are 10 μm and 20 μm respectively using the 240 kHz FDML laser, and 12 μm and 20 μm respectively using the 480 kHz FDML laser. 3D-OCT datasets were acquired by pulling back the catheter with 2mm/s pull-back speed. Using this high speed imaging system, one 8 Gigabyte dataset can be acquired in 8 seconds, corresponding to a 16mm pull-back range and ~4,000 frames. By increasing the pull-back speed of the catheter, the imaging range can be even larger. Figure 3 shows *in vivo* 3D volumetric OCT dataset from a human finger with 240 kHz axial line rate. Figs. 3 (A) and (B) show the 3D rendering and the *en face* view of the finger. Figs. 3 (C) and (D) show cross-sectional images along the fast scan direction during the pull back and Fig. 3 (E) shows the cross-sectional image along the pull back direction. The stratum corneum, sweat ducts, and fingerprint ridges can be clearly delineated. With higher line rate, one OCT image can include more lines with the same imaging frame rate, which can improve the image quality and show more features in the tissues. Figure 4 shows an example OCT images from the finger with 480 kHz axial line rate. Fig. 4 (A) and (B) show the *en face* view of the finger at different imaging depth. Sweat ducts can be seen distributed on the surface of the finger. Fig. 3 (C) shows the cross-sectional image along the fast scan direction during the pull back and Fig. 3 (E) shows the cross-sectional image along the pull back direction. Fig. 3 (D) shows the

3D rendering of the dataset. With twice more pixels in the cross-sectional image, more detail structures can be clearly distinguished in the finger.

Figure 5 shows an example 3D dataset of the freshly excised human colon. Fig. 5 (A) shows the *en face* view of the colon at the depth of 250 μm, where the distributed crypt structure can be clearly seen. Figs. 5 (B) and (C) show the cross-sectional images along the PZT scan direction and pull-back direction, respectively. In fig. 5 (C), the lamina propria layer can be distinguished underneath the epithelium layer with crypt structure, showing deep penetration range of this imaging system. In this dataset, a 2 mm x 6.5 mm x 1.65 mm volumetric dataset was recorded in 3.25 seconds with 1,531 frames in total, demonstrating the high speed, large-area imaging, and dense sampling capability of the imaging system.
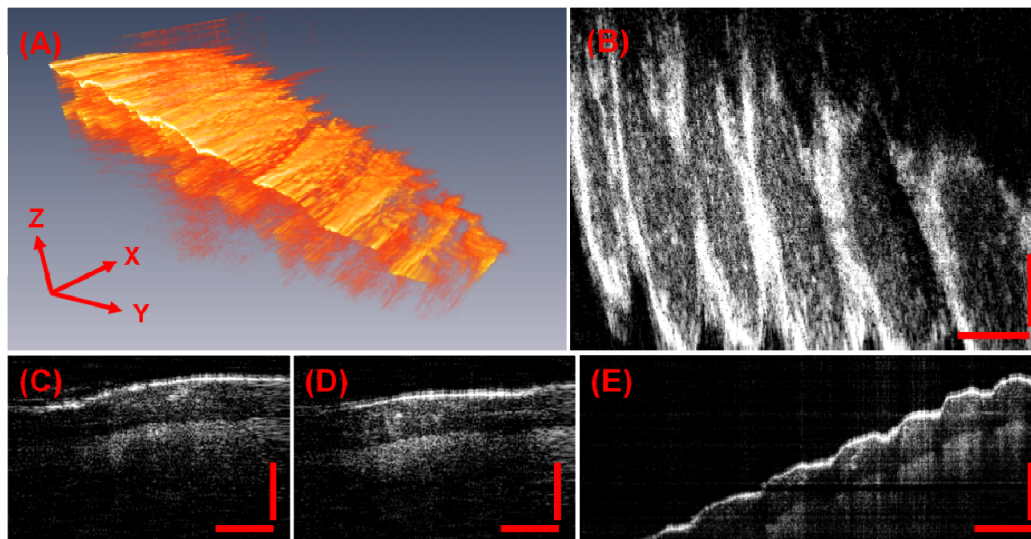

Figure 3. 3D volumetric OCT images from a human finger using 240 kHz FDML laser. (A) 3D rendering. (B) *En face* view through fingerprint ridges. (C-D) Cross-sectional images at different time points during the pull back. (E) Cross-sectional images along the pull back direction. Scale bar: 500μm.
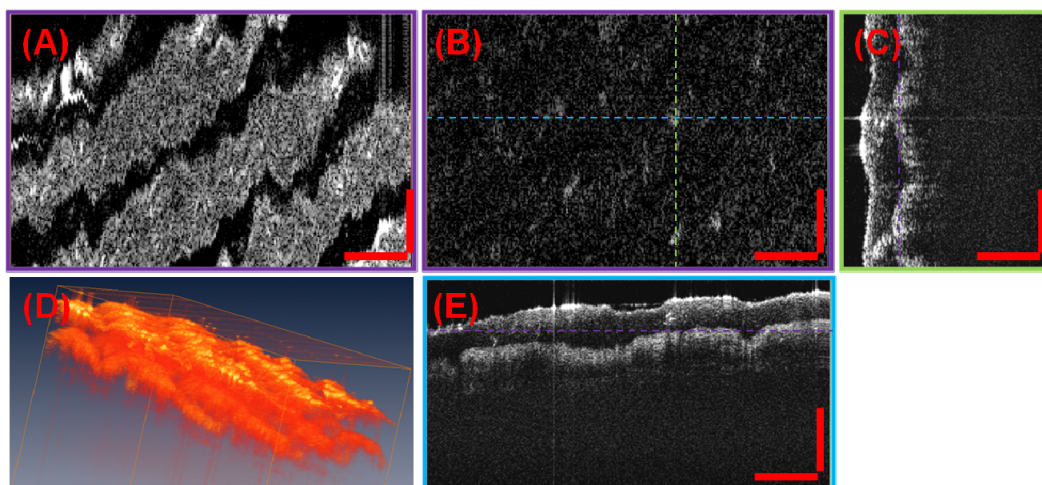

Figure 4. 3D volumetric OCT images from a human finger using 480 kHz FDML laser. (A) *En face* view through fingerprint ridges.3D (B) *En face* view 500 μm deeper than (A). (C) Cross-sectional image in the fast scan direction. (D) 3D rendering. (E) Cross-sectional image along the pull back direction. Scale bar: 500 μm.
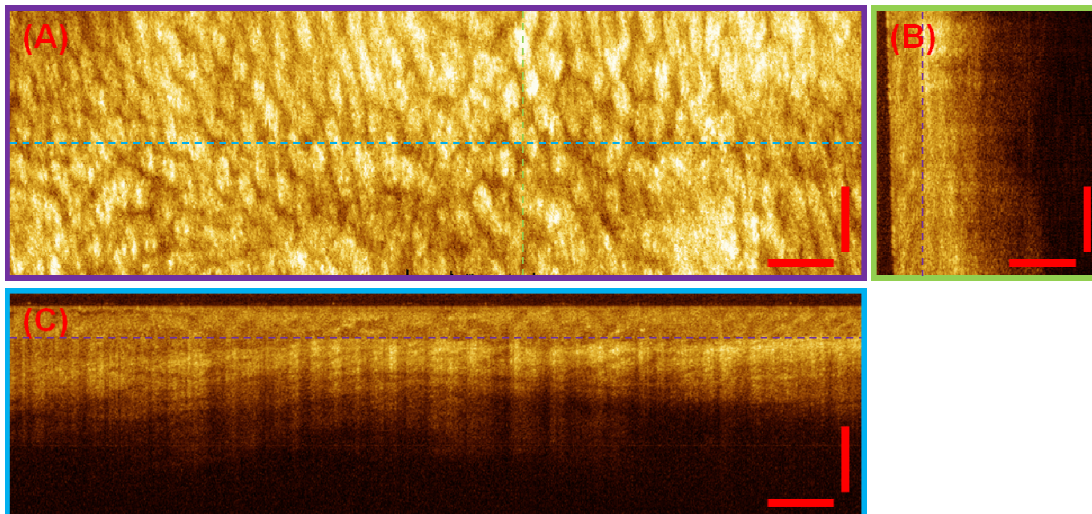
Figure 5. 3D volumetric OCT images from a fresh excised human colon using 480 kHz FDML laser. (A) *En face* view of the colon at the depth of 300 μm. (B) Cross-sectional image in the fast scan direction. (C) Cross-sectional image along the pull-back direction. Scale bar: 500 μm.

In conclusion, we developed a PZT based miniature catheter with an outer diameter of 3mm for ultrahigh speed endoscopic OCT using an FDML laser at 240 and 480 kHz axial scan rate. OCT imaging with up to 6.5 mm imaging range, 10 μm axial resolution, 20μm lateral resolution, and frame rate of 480 fps is demonstrated. The miniaturized PZT bender not only can achieve high scanning speed but allows integration with different slow scan mechanisms, providing a variety of imaging patterns for different endoscopic applications.

Acknowledgement

References

[1] D. Huang, E. A. Swanson, C. P. Lin, J. S. Schuman, W. G. Stinson, W. Chang, M. R. Hee, T. Flotte, K. Gregory, C. A. Puliafito, and J. G. Fujimoto, "OPTICAL COHERENCE TOMOGRAPHY," *Science,* vol. 254, pp. 1178-1181, Nov 1991.
[2] G. J. Tearney, S. A. Boppart, B. E. Bouma, M. E. Brezinski, N. J. Weissman, J. F. Southern, and J. G. Fujimoto, "Scanning single-mode fiber optic catheter-endoscope for optical coherence tomography," *Optics Letters,* vol. 21, pp. 543-545, Apr 1996.
[3] G. J. Tearney, M. E. Brezinski, B. E. Bouma, S. A. Boppart, C. Pitris, J. F. Southern, and J. G. Fujimoto, "In vivo endoscopic optical biopsy with optical coherence tomography," *Science,* vol. 276, pp. 2037-2039, 1997.
[4] D. C. Adler, Y. Chen, R. Huber, J. Schmitt, J. Connolly, and J. G. Fujimoto, "Three-dimensional endomicroscopy using optical coherence tomography," *Nature Photonics,* vol. 1, pp. 709-716, Dec 2007.
[5] M. J. Suter, P. A. Jillella, B. J. Vakoc, E. F. Halpern, M. Mino-Kenudson, G. Y. Lauwers, B. E. Bouma, N. S. Nishioka, and G. J. Tearney, "Image-guided biopsy in the esophagus through comprehensive optical frequency domain imaging and laser marking: a study in living swine," *Gastrointest Endosc,* vol. 71, pp. 346-53, 2010 Feb (Epub 2009.
[6] G. J. Tearney, S. Waxman, M. Shishkov, B. J. Vakoc, M. J. Suter, M. I. Freilich, A. E. Desjardins, W.-Y. Oh, L. A. Bartlett, M. Rosenberg, and B. E. Bouma, "Three-dimensional coronary artery microscopy by intracoronary optical frequency domain imaging," *JACC Cardiovasc Imaging,* vol. 1, pp. 752-61, 2008 2008.

[7] A. Sergeev, V. Gelikonov, G. Gelikonov, F. Feldchtein, R. Kuranov, N. Gladkova, N. Shakhova, L. Snopova, A. Shakhov, I. Kuznetzova, A. Denisenko, V. Pochinko, Y. Chumakov, and O. Streltzova, "In vivo endoscopic OCT imaging of precancerand cancer states of human mucosa," *Opt. Express,* vol. 1, pp. 432-440, 1997.

[8] A. D. Aguirre, J. Sawinski, S. W. Huang, C. Zhou, W. Denk, and J. G. Fujimoto, "High speed optical coherence microscopy with autofocus adjustment and a miniaturized endoscopic imaging probe," *Optics Express,* vol. 18, pp. 4222-4239, Mar 2010.

[9] X. M. Liu, M. J. Cobb, Y. C. Chen, M. B. Kimmey, and X. D. Li, "Rapid-scanning forward-imaging miniature endoscope for real-time optical coherence tomography," *Optics Letters,* vol. 29, pp. 1763-1765, Aug 2004.

[10] W. Jung, D. T. McCormick, J. Zhang, L. Wang, N. C. Tien, and Z. P. Chen, "Three-dimensional endoscopic optical coherence tomography by use of a two-axis microelectromechanical scanning mirror," *Applied Physics Letters,* vol. 88, p. 3, Apr 2006.

[11] K. H. Kim, B. H. Park, G. N. Maguluri, T. W. Lee, F. J. Rogomentich, M. G. Bancu, B. E. Bouma, J. F. de Boer, and J. J. Bernstein, "Two-axis magnetically-driven MEMS scanning catheter for endoscopic high-speed optical coherence tomography," *Optics Express,* vol. 15, pp. 18130-18140, Dec 2007.

[12] Y. T. Pan, H. K. Xie, and G. K. Fedder, "Endoscopic optical coherence tomography based on a microelectromechanical mirror," *Optics Letters,* vol. 26, pp. 1966-1968, Dec 2001.

[13] J. J. Sun, S. G. Guo, L. Wu, L. Liu, S. W. Choe, B. S. Sorg, and H. K. Xie, "3D In Vivo optical coherence tomography based on a low-voltage, large-scan-range 2D MEMS mirror," *Optics Express,* vol. 18, pp. 12065-12075, Jun 2010.

[14] W. Wieser, B. R. Biedermann, T. Klein, C. M. Eigenwillig, and R. Huber, "Multi-Megahertz OCT: High quality 3D imaging at 20 million A-scans and 4.5 GVoxels per second," *Opt. Express,* vol. 18, pp. 14685-14704, 2010.